Published in final edited form as:
Hepatology. 2010 December ; 52(6): 2001–2011. doi:10.1002/hep.23941.

Rosiglitazone Attenuates Age- and Diet-associated Nonalcoholic Steatohepatitis in male LDL receptor knockout mice

Anisha A. Gupte[1], **Joey Z. Liu**[1], **Yuelan Ren**[1], **Laurie J. Minze**[1], **Jessica R. Wiles**[1], **Alan R. Collins**[1], **Christopher J. Lyon**[1], **Domenico Pratico**[3], **Milton J. Finegold**[4], **Stephen T. Wong**[2], **Paul Webb**[1], **John D. Baxter**[1], **David D. Moore**[5], and **Willa A. Hsueh**[1]

[1]The Methodist Hospital Research Institute, Center for Diabetes Research, Weill Cornell Medical College, Houston, TX 77030, USA

[2]The Methodist Hospital Research Institute, Center for Bioengineering and Informatics, Weill Cornell Medical College, Houston, TX 77030, USA

[3]Temple University School of Medicine, Department of Pharmacology, Philadelphia, PA 19140, USA

[4]Texas Children's Hospital, Department of Pathology, Houston, TX 77030, USA

[5]Baylor College of Medicine, Department of Molecular and Cellular Biology, Houston, Texas 77030, USA

Abstract

Nonalcoholic fatty liver disease (NAFLD) is a common complication of obesity that can progress to nonalcoholic steatohepatitis (NASH), a serious liver pathology that can advance to cirrhosis. The mechanisms responsible for NAFLD progression to NASH remain unclear. Lack of a suitable animal model that faithfully recapitulates the pathophysiology of human NASH is a major obstacle in delineating mechanisms responsible for progression of NAFLD to NASH and, thus, development of better treatment strategies. We identified and characterized a novel mouse model, middle-aged male *LDLR*$^{-/-}$ mice fed high-fat diet (HFD), which developed NASH associated with 4 of 5 metabolic syndrome (MS) components. In MS mice, as observed in humans, liver steatosis and oxidative stress promoted NASH development. Aging exacerbated the HFD-induced NASH such that liver steatosis, inflammation, fibrosis, oxidative stress and liver injury markers were greatly enhanced in middle-aged versus young *LDLR*$^{-/-}$ mice. While expression of genes mediating fatty acid oxidation and antioxidant responses were upregulated in young *LDLR*$^{-/-}$ mice fed HFD, they were drastically reduced in MS mice. However, similar to recent human trials, NASH was partially attenuated by an insulin-sensitizing peroxisome proliferator-activated receptor-gamma (PPARγ) ligand, rosiglitazone. In addition to expected improvements in MS, newly identified mechanisms of PPARγ ligand effects included stimulation of antioxidant gene expression and mitochondrial β-oxidation, and suppression of inflammation and fibrosis. LDLR-deficiency promoted NASH, since middle-aged C57BL/6 mice fed HFD did not develop severe inflammation and fibrosis, despite increased steatosis.

Conclusion—MS mice represent an ideal model to investigate NASH in the context of MS, as commonly occurs in human disease, and NASH development can be substantially attenuated by PPARγ activation, which enhances β-oxidation.

Corresponding author: Willa A. Hsueh, MD, wahsueh@tmhs.org, 713-441-2520 (phone), 713-793-7162 (fax).

Keywords

NASH; aging; oxidative stress; Nrf2; Rosiglitazone; chronic liver disease; mitochondrial dysfunction; *LDLR*−/−

NASH is the most common liver disease in the Western world, affecting more than 18% of obese individuals (1). NASH is strongly associated with insulin resistance, and nearly five out of six NASH patients have the metabolic syndrome (MS) (2). NASH can progress to cirrhosis, but despite its severity and prevalence, there are no approved treatments for NASH. However, the recent PIVENS trial demonstrated improvement in NASH histology with either vitamin E or the insulin-sensitizing PPARγ ligand, pioglitazone (PIO) (3). The vitamin E effect underscored the critical role of oxidative stress in NASH but occurred in the *absence* of an improvement in insulin sensitivity, demonstrating an unexpected dissociation between NASH and insulin resistance and raising questions about the mechanism of action of PIO. PPARγ ligand effects, independent of insulin sensitization, thus warrant further examination in the context of NASH. A major barrier to better understanding PPARγ mechanisms in NASH is the lack of a suitable animal model that mimics the pathophysiology of human NASH.

We recently identified and phenotyped a 'MS mouse', middle-aged (12-month-old) male *LDLR*$^{-/-}$ mice fed 3 months of HFD, that developed 4 of 5 criteria of human MS (4). These mice not only developed worse MS and diabetes than HFD-fed young (3-month-old) *LDLR*$^{-/-}$ mice, but also developed worse atherosclerosis, which correlated with a profound failure of vascular antioxidant defense systems (4). Since a 'two-hit' theory has been proposed for the progression of NAFLD to NASH: hepatic steatosis associated with MS being the first hit, followed by a second insult from increased oxidative stress (5), we hypothesized that the MS mouse represents a useful model of the progression of NAFLD to NASH. We report herein that MS mice developed NASH with all the histologic characteristics of human disease, including age-dependency and attenuation in response to treatment with the PPARγ ligand rosiglitazone (RSG). Newly identified actions of RSG included reduction of liver oxidative stress by up-regulation of expression of nuclear factor-(erythroid-derived 2)-like 2 *(Nrf2)*, a "master" regulator of the anti-oxidant response, stimulation of liver mitochondrial fatty acid β-oxidation, and inhibition of inflammation and fibrosis, all of which appear independent of its systemic insulin-sensitizing effects. These observations have implications for development of new strategies to prevent and treat this increasingly common cause of end stage liver disease.

EXPERIMENTAL PROCEDURES

Animals and treatments

Male *LDLR*$^{-/-}$ mice (Jackson Laboratory, Bar Harbor, ME) were group-housed in microisolator cages with a 12 hour light and dark cycle. Young (3 months-of-age) and middle-aged (12 months-of-age) mice were randomly assigned to 3 months of standard chow diet (Harlan Teklad, Madison, WI) or a high-fat, high-cholesterol Western diet (HFD, Research Diets, New Brunswick, NJ, 41 kcal% fat and 0.15% cholesterol) or HFD supplemented with RSG (1.2 g RSG/kg of HFD). Body fat was measured by Nuclear Magnetic Resonance (NMR, Echo Medical Systems, Houston, TX). Mice were sacrificed after 12 weeks of diet, following an overnight fast. All protocols were approved by the Institutional Animal Care and Use Committee (IACUC) of The Methodist Hospital Research Institute and carried out in accordance with the NIH Guide for the Care and Use of Laboratory Animals.

Histopathology

Formalin-fixed liver tissue was processed for histological analyses and stained with Haematoxylin and Eosin or with Masson's Trichrome to detect collagen for fibrosis analyses. Steatosis, fibrosis and inflammation were quantified under the guidance of Dr. Finegold, according to the guidelines of Kleiner et al. for NASH diagnosis (6). Steatosis (lipid vesicles/lobule area) and inflammation (foci/lobule) were quantified at 40× and 200× magnification, respectively, using Nikon NIS-Elements AR 3.0 software.

RNA purification, cDNA synthesis and qRT-PCR

Gene expression was performed as previously described and normalized to *GAPDH* expression (4).

Metabolic analyses

Plasma lipids, and alanine aminotransferase (ALT) and aspartate aminotransferase (AST) levels were analyzed by the Yale and Cincinnati Mouse Metabolic Phenotyping Centers (MMPC).

Mitochondrial isolation and functional analyses

Liver mitochondria were isolated by differential centrifugation as previously described (7), and mitochondrial function was assessed on a Clark-type electrode (Strathkelvin MT-100, N Lanarkshire, Scotland) by respirometry, using 1 mg/ml isolated mitochondria and sequential addition of substrate (glutamate malate, succinate or palmitoyl carnitine,5 mM) and ADP (150 μM) to measure mitochondrial states 2, 3 and 4 respiration.

Laser capture microdissection (LCM) analyses

Liver tissue was frozen with Tissue-Tek® O.C.T. Compound (Electron microscopy sciences, Hatfield, PA) and 8 μM sections were rapidly stained using HistoGene® LCM Frozen Section Staining Kit (Molecular Devices, Sunnyvale, CA). LCM was performed using Arcturus$^{XT™}$ Microdissection System (Molecular devices). RNA was extracted using PicoPure® RNA Isolation Kits (Molecular devices) and subjected to quantitative RT-PCR.

Oxidative stress quantification

Liver tissue was minced and homogenized in PBS containing 0.01% butylated hydroxytoluene and 0.77mM EDTA. Total lipids were extracted with Folch solution (66% methanol:33% chloroform), and extracts assayed for F2α-isoprostane (4).

Statistical Analyses

All data are presented as ±SE. Differences between groups were analyzed using one way analysis of variance (ANOVA) or student's t-test as appropriate. Differences between individual means were determined using Tukey's LSD. Statistical significance was set at $P<0.05$.

RESULTS

Middle-aged, but not young, HFD-fed *LDLR*$^{-/-}$ mice develop NASH, which is attenuated by RSG

We have previously shown that middle-aged *LDLR*$^{-/-}$ mice developed worse MS than their younger counterparts when fed HFD (greater fasting blood glucose, insulin, triglyceride concentrations; reduced HDL cholesterol; and higher oxidative stress), despite similarly increased cholesterol levels, and that RSG improved all these MS components (4). In the

present investigation, middle-aged *LDLR*$^{-/-}$ mice fed HFD gained substantially more body and liver fat than young mice, and had markedly increased plasma phospholipids, which are associated with type 2 diabetes (8); hepatic F2α-isoprostane levels, an indicator of liver oxidative stress; and plasma ALT and AST concentrations, common markers of liver injury (Fig. 1A–F). RSG did not alter the HFD-induced body fat increase (Fig. 1A), but substantially decreased liver fat, plasma phospholipids, ALT and AST, and liver F2α-isoprostane in both groups (Fig. 1B–F).

In agreement with NMR-measured liver fat, chow-fed middle-aged *LDLR*$^{-/-}$ mice developed histologic microsteatosis. However, HFD-fed young mice developed marked steatosis, and MS mice developed massive micro- and macrovesicular steatosis (Fig. 2A; Fig. 3A). RSG almost completely attenuated steatosis in HFD-fed young mice, but had a strikingly zonal effect on steatosis clearance in MS mice, demonstrating a 'snowflake' pattern due to complete lipid clearance in periportal but not perivenous regions of the liver (Fig. 2A). The numbers of inflammatory foci in chow-fed middle-aged mice were similar to those of HFD-fed young mice, but greatly increased with HFD (Fig. 2B; Fig. 3B). RSG treatment partially attenuated HFD-induced inflammatory foci in MS mice. While chow-fed young and middle-aged mice and HFD-fed young mice demonstrated similar portal vein collagen expression, HFD markedly increased sinusoidal fibrosis in middle-aged mice, which was completely attenuated by RSG treatment (Fig. 2D, Fig. 3C). Only MS mice revealed hepatocyte ballooning, which was partially masked by macrosteatosis, but completely attenuated by RSG treatment (Fig. 3D,E).

NASH diagnosis in humans is determined by histological scoring to quantify liver steatosis, inflammation, hepatocyte injury and extent and location of fibrosis (6). MS mice faithfully recapitulated human NASH, developing all the histologic hallmarks of human disease, and responding to PPARγ activation (Fig. 3A–E), recently shown to be effective in MS patients with NASH (3).

MS mice have altered liver expression of metabolic, pro-inflammatory, and pro-fibrotic genes

To understand the mechanisms underlying NASH in the MS mouse, we investigated liver expression of key genes mediating lipid metabolism, inflammation and fibrosis. HFD-fed young mice revealed lipid metabolism gene expression changes consistent with increased mitochondrial β-oxidation (e.g. increased expression of *HADHA* and *ACADm*, Fig. 4A). In sharp contrast, MS mice showed the opposite pattern: decreased expression of the β-oxidation genes *HADHA and ACADm*; reduced expression of *CPT1A*, a rate-limiting mitochondrial lipid transporter; and dramatically increased expression of *ACC2*, a negative regulator of *CPT1A* activity, suggesting that a marked β-oxidation deficiency could contribute, at least in part, to hepatic steatosis in MS mice. RSG treatment suppressed *ACC2* expression and increased *CPT1A, HADHA* and *ACADm* expression in MS mice, consistent with an effect to increase β-oxidation.

HFD also increased SREBP1c expression (Fig. 4B), a master regulator of lipogenic gene expression, in both young and middle-aged mice, but did not increase expression of the lipid synthesis genes *FASN or DGAT*. RSG treatment increased *SREBP1c*, *FASN* and *DGAT1* in HFD-fed middle-aged mice, consistent with previous reports in mice and humans that PPARγ activation can increase *de novo* lipogenesis (DNL (9)). These data suggest that the RSG effect to stimulate DNL is offset by an increase in fatty acid β-oxidation to attenuate hepatic steatosis.

Chronic inflammation is an important component of NASH distinguishing it from relatively benign NAFLD. Liver expression of pro-inflammatory genes, including *CD68* (a marker of

macrophage accumulation), *MCP-1*, osteopontin (*OPN*) and *TNFα* showed an age- and HFD-associated increase, although middle-aged mice had roughly twice the pro-inflammatory gene expression of young mice, consistent with histologic changes (Fig. 4C). RSG treatment generally decreased gene expression of these HFD-induced inflammatory markers in both young and middle-aged mice.

Fibrosis is a critical predictor of NASH progression to cirrhosis (10). Key pro-fibrotic genes, including *TGF1β*, a profibrotic cytokine, and collagens I and IV were increased in expression by HFD in both age groups, but markedly more so in middle-aged vs. young mice (Fig. 4D). RSG treatment tended to decrease *TGF1β* and collagen IV, and markedly decreased the dramatic increase in collagen I expression in MS mice, suggesting that RSG has anti-fibrotic effects.

Taken together, MS mice demonstrate liver gene expression changes indicative of reduced β-oxidation and increased inflammation and fibrosis, paralleling the histologic changes, which are rescued by RSG treatment.

Middle-aged mice have attenuated liver antioxidant responses to HFD

MS mice demonstrated robust oxidative stress implicated to drive progression of NAFLD to NASH. Chow-fed young and middle-aged mice demonstrated similar liver *Nrf2* expression, but showed minor (1.3 to 1.6 fold) age-associated increases in the antioxidant response genes *NQO1*, *SOD2* and catalase (Fig. 4E). In young mice, HFD increased *Nrf2, SOD2* and catalase expression. Surprisingly, HFD did not increase *Nrf2* expression in middle-aged mice and ***decreased*** expression of these *Nrf2*-regulated genes, despite a marked increase in liver oxidative stress. RSG strongly induced *Nrf2* transcription in MS mice, resulting in expression similar to that of young HFD-fed mice, and blocked HFD-induced repression of *NQO1, SOD2* and catalase. Thus, MS mice exhibit a profound failure to upregulate liver antioxidant genes in response to HFD, paralleling their defective vascular antioxidant response (4). Moreover, RSG treatment rescued both hepatic and vascular *Nrf2* pathway gene expression in MS mice to reduce tissue oxidative stress, thereby contributing to the attenuation of both NASH and accelerated atherosclerosis.

Rosiglitazone treatment improves liver mitochondrial function in MS mice

To determine whether gene expression changes with HFD and RSG correspond to mitochondrial functional alterations, we analyzed isolated liver mitochondria of young and middle-aged $LDLR^{-/-}$ mice for differences in respiratory efficiency (ATP/O: ATP produced per molecule of O_2 consumed) and respiratory control ratios (RCR: state3 (substrate3 driven respiration)/state2 (substrate-driven respiration)) using palmitoyl carnitine as a representative fatty acid substrate. Liver mitochondria of chow- and HFD-fed middle-aged mice had lower ATP/O ratios than those of young mice (Fig. 5A). HFD did not decrease ATP/O ratios in either age group, but RSG tended to increase the ATP/O ratio of HFD-fed middle-aged but not young mice, resulting in similar values among the two age groups. Thus, the age-associated decline in respiration efficiency was not worsened by HFD and could be normalized by RSG.

State 3 palmitoyl carnitine respiration, indicative of mitochondrial fatty acid β-oxidation, tended to increase in HFD-fed young mice, but substantially decreased in MS mice. This decrease was prevented by RSG (Fig. 5B). These state 3 changes contributed to similar RCR changes, which mirrored alterations in liver genes associated with fatty acid β-oxidation (*ACC2*, *CPT1A*, *HADHA*, and *ACADm*), suggesting that RSG exerts its effects on liver β-oxidation through restoring appropriate HFD-induced up-regulation of these genes. RCRs of

two non-fatty-acid mitochondrial substrates, glutamate/malate and succinate, were not significantly altered by HFD in either age group (data not shown).

Liver mitochondria were analyzed for expression of *Cox5a*, an important electron transport chain (ETC) component, to evaluate potential mechanisms responsible for age- and diet-associated changes in fatty acid oxidation. Cox5a expression was similar in chow-fed mice of both age groups, increased with HFD in young mice, but decreased in MS mice. RSG increased *Cox5a* only in MS mice, normalizing expression to that of HFD-fed young mice (Fig. 5D). Thus, an age-associated deficit in HFD-induced expression of one or more ETC components may result in increased oxidative stress, which is reversed by RSG treatment.

Although RSG attenuated steatosis in MS mice, there was a marked difference in periportal vs. perivenular steatosis, creating a 'snowflake pattern' of steatosis following RSG treatment (Fig. 2A). Previous evidence suggested that there are zonal variations in hepatocyte function (11), which could explain this phenotype. We therefore employed LCM to collect periportal and perivenular liver regions of MS mice with or without RSG treatment in order to analyze regional gene expression differences. RSG treatment preferentially increased periportal vs. perivenous *CPT1A* and *ACADm* expression (Fig. 6A–B), suggesting that regional differences in RSG-mediated β-oxidation responses could explain the steatosis pattern. In contrast, RSG similarly decreased both periportal and perivenular pro-inflammatory *MCP-1* expression, and dramatically reduced the marked increase in perivenular-specific pro-inflammatory *OPN* expression (Fig. 6C–D). Thus, regional differences in RSG responses were apparently not due to differential RSG distribution in the affected areas.

LDLR-deficiency promotes age-associated liver inflammation and fibrosis

LDLR-deficiency, age and HFD all contributed to NASH development in MS mice. In order to address the relative contribution of *LDLR*-deficiency, we examined liver responses to HFD in middle-aged C57BL/6 vs. $LDLR^{-/-}$ mice. Both strains gained similar weight after 3 months of HFD, but only the $LDLR^{-/-}$ mice revealed HFD-induced triglyceride increases and HDL decreases (Fig. S1A, B). Surprisingly, however, HFD-fed C57BL/6 mice had slightly more liver steatosis and NMR-determined liver fat and significantly more microsteatosis than HFD-fed $LDLR^{-/-}$ mice (Fig. S1E), despite similar plasma AST and ALT increases (Fig. S1C, D), suggesting that both experienced similar HFD-induced liver injury. Plasma cholesterol was increased in $LDLR^{-/-}$ vs. C57BL/6 chow-fed mice, and further increased in both groups upon HFD (Fig. 7A). Pro-inflammatory (*MCP1*, *TNFα*, *CD68*, Fig. 7B–D) and profibrotic (collagen1α2 and collagen4α1, Fig. 7E–F) gene expression was similar in chow-fed $LDLR^{-/-}$ and C57BL/6 mice. HFD markedly increased pro-inflammatory and profibrotic gene expression in both genotypes, but changes were substantially greater in $LDLR^{-/-}$ vs. C57Bl/6 mice (Fig. 7B–F). Numbers of inflammatory foci per lobule were 67% greater in HFD-fed $LDLR^{-/-}$ mice than C57BL/6 mice (HFD-C57BL/6 1.4 ±0.26, HFD-$LDLR^{-/-}$ 2.33±0.28, $P<0.05$), consistent with results from *in vitro* cultures of isolated C57BL/6 and $LDLR^{-/-}$ mouse hepatocytes, in which $LDLR^{-/-}$ hepatocytes revealed 5-fold or greater *MCP1*, *TNFα* and *IL1*-β gene expression than C57BL/6 hepatocytes (Fig. S1F–I). Thus, *LDLR* deficiency markedly accentuated effects of HFD on pro-inflammatory and profibrotic gene expression in middle-aged mice, highlighting the contribution of hypercholesterolemia.

DISCUSSION

The MS mouse (HFD-fed, middle-aged $LDLR^{-/-}$ mouse) recapitulates all of the major characteristics of human NASH, including steatosis, ballooning degeneration, inflammation and fibrosis, underscoring the importance of oxidative stress and aging, which mediate liver injury in humans. Indeed, the livers of middle-aged mice exhibited mitochondrial

dysfunction and, in the presence of HFD, defects in β-oxidation and a generalized decrease in antioxidant gene responses. Similar to PPARγ ligand effects on human NASH (3,12), RSG substantially attenuated histologic endpoints and decreased elevated serum enzyme levels in MS mice, likely, at least partially due to improvements in MS. Since activation of PPARγ in the liver increases DNL, there have been concerns about worsening of steatosis and liver injury when PPARγ ligands are administered to patients with NASH (9). However, our results indicate that PPARγ activation induced novel, previously undefined, mechanisms to attenuate NASH, including improved β-oxidation to reduce hepatic steatosis and upregulation of the *Nrf2* pathway to decrease oxidative stress to override the PPARγ-induced DNL effects.

Mice fed methionine-choline-deficient (MCD) diet are a commonly used model of NASH because they develop severe liver inflammation and fibrosis (13). However, MCD-fed mice do not develop MS, instead demonstrating reductions in body weight and plasma triglycerides (14). Conversely, hyperphagic ob/ob and db/db mice develop MS and liver steatosis, but not hepatic inflammation and fibrosis, possibly due to their loss of normal leptin signaling (15). MS mice described in herein develop obesity, diabetes and dyslipidemia, concurrent with histologic NASH, allowing the investigation of MS-related mechanisms involved in the pathogenesis and treatment of NASH.

NASH and atherosclerosis share multiple risk factors including obesity, hyperlipidemia, diabetes, oxidative stress, and elevated plasma AST and ALT (16,17). Elevated cholesterol, rather than steatosis *per se*, causes hepatic inflammation in mice and has been proposed to play a similar role in humans (18). Metabolomic studies further suggest a role for cholesterol, since progressive increases in *both* liver saturated fatty acid and cholesterol content accompany the progression of normal livers to NAFLD to NASH (19). Recently, the *LDLR*$^{-/-}$ mouse, a widely-used hypercholesterolemic atherosclerosis model, has been suggested as a NASH model because it develops liver inflammation not present in normocholesterolemic mice (20). Indeed, we found that age- and gender-matched HFD-fed C57BL/6 mice that do not develop hypercholesterolemia, had slightly more steatosis, but much less inflammation and fibrosis than MS mice. Liver triglyceride accumulation does not by itself cause hepatic inflammation, since inhibition of liver triglyceride synthesis to decrease steatosis was still associated with markedly increased liver inflammation and fibrosis (21). Based on the results of Bieghs et al. (22), Kupffer cell activation in response to HFD-induced dyslipidemia via SRA or CD36 may be partially responsible for the increased inflammation, fibrosis and oxidative stress in MS mice.

Age is an independent risk factor for bridging fibrosis in humans, although the mechanism of this age effect is currently unknown (23,24). The MS mouse also demonstrates a critical role of age in development of NASH, exhibiting age-related defects in liver mitochondrial function and antioxidant capacity. Livers of HFD-fed young *LDLR*$^{-/-}$ mice revealed increased β-oxidation and an enhanced antioxidant response. These ‘adaptations’ to HFD likely protected the liver from oxidative stress and subsequent inflammation and injury. In contrast, middle-aged *LDLR*$^{-/-}$ mice lacked this capacity, failing to increase liver mitochondria RCR in response to HFD with decreased palmitoyl carnitine-induced state 3 respiration (β-oxidation), ATP:O ratios, and β-oxidation-related gene expression: *all* suggestive of decreased mitochondrial efficiency. Middle-aged mice, unlike young mice, also failed to up-regulate mitochondrial ETC gene expression (e.g. complex IV *Cox5a*) in response to HFD. Previous studies have shown that mitochondria of aging animals display multiple ETC abnormalities, reduced ATP generation capacity and decreased complex I and IV activities (26). Complex IV, which passes electrons to water in the final step of the mitochondrial ETC, is particularly susceptible to oxidative stress, and ROS generated by dysfunctional mitochondria can result in further damage and increased ROS production (25).

RSG-induced decreases in oxidative stress may prevent Complex IV damage, as supported by an increase in *Cox5a* expression in RSG treated MS mice, and contribute to improved mitochondrial function and increased β-oxidation. More detailed studies are needed to dissect the potential mitochondrial protective effects of PPARγ activation in aging.

The importance of β-oxidation for RSG-mediated prevention of steatosis was supported by gene expression results using LCM. RSG differentially altered steatosis regionally in MS mouse livers; steatosis improved primarily in periportal areas, leaving a “snowflake” pattern of persistent steatosis in perivenular areas. Consistent with this histologic pattern, we found increased expression of β-oxidation genes in periportal areas of RSG-treated MS mice, with no increase in perivenular areas, thus paralleling the steatosis pattern. Periportal regions reportedly have greater expression of fatty acid metabolism and gluconeogenic genes, whereas perivenous areas have greater lipogenic and glycolytic gene expression (11).

Age- and HFD-associated deficits in the *Nrf2* pathway, a key regulator of antioxidant gene expression, corresponded with increased liver oxidative stress. Similar to the liver, decreased vascular expression of Nrf2-regulated antioxidant enzymes in MS mice was associated with markedly accelerated atherosclerosis, and both were prevented by RSG (4). *Nrf2*-deficient mice fed MCD diet developed worse steatosis, inflammation and fibrosis than wild-type controls (26,27), while HFD increased liver oxidative stress in $Nrf2^{-/-}$ but not wild-type mice (28). These results, thus, support the importance of *Nrf2* activity in modulating NASH and opposing HFD-induced ROS generation. The combination of aging and metabolic stress, as occurs in the MS mouse, appears to induce mitochondrial dysfunction and impair antioxidant responses, resulting in excess oxidative stress and tissue injury. Our data indicate HFD is particularly harmful in the aging animal, and suggest that improvements in *Nrf2* pathway activity can attenuate HFD-induced damage.

Despite the high prevalence of NASH and its potential for progression to end-stage liver disease, there are no approved treatments for NASH. Although recent Vitamin E and PPARγ ligand trials demonstrated positive effects, substantial unabated disease remains (3,12,29). The present investigation demonstrates that RSG induces several hepatic mechanisms to attenuate NASH, including improved β-oxidation and mitochondrial function to decrease steatosis, suppression of pro-inflammatory and pro-fibrotic genes, and stimulation of Nrf2 and downstream antioxidants to decrease oxidative stress. Further studies in this novel mouse model will be necessary to define the relative importance of each of these mechanisms to attenuate liver injury, and should provide valuable insight into the development of new treatments for NASH.

Supplementary Material

Refer to Web version on PubMed Central for supplementary material.

ABBREVIATIONS

LDLR	Low density lipoprotein receptor
RSG	rosiglitazone
Nrf2	nuclear factor-(erythroid-derived 2)-related factor 2
ALT	alanine aminotransferase
AST	aspartate aminotransferase
CPT1A	carnitine palmitoyltransferase 1a

DNL	*de novo* lipogenesis
LCM	laser capture microdissection
ROS	reactive oxygen species

Acknowledgments

The authors thank William Widger, Luz Vela and Kristina Henkel (University for Houston) for technical assistance with mitochondrial respiration studies, and thank Candace Fenno, Aijun Zhang, Xuefeng Xia and Tuo Deng for technical assistance and scientific advice. This study was supported by R01 HL075171 to WAH.

REFERENCES

1. Turkish AR. Nonalcoholic fatty liver disease: emerging mechanisms and consequences. Curr Opin Clin Nutr Metab Care. 2008; 11:128–133. [PubMed: 18301087]
2. Chitturi S, Abeygunasekera S, Farrell GC, Holmes-Walker J, Hui JM, Fung C, Karim R, et al. NASH and insulin resistance: Insulin hypersecretion and specific association with the insulin resistance syndrome. Hepatology. 2002; 35:373–379. [PubMed: 11826411]
3. Sanyal AJ, Chalasani N, Kowdley KV, McCullough A, Diehl AM, Bass NM, Neuschwander-Tetri BA, et al. Pioglitazone, Vitamin E, or Placebo for Nonalcoholic Steatohepatitis. N Engl J Med. 2010 Epub.
4. Collins AR, Lyon CJ, Xia X, Liu JZ, Tangirala RK, Yin F, Boyadjian R, et al. Age-accelerated atherosclerosis correlates with failure to upregulate antioxidant genes. Circ Res. 2009; 104:e42–e54. [PubMed: 19265038]
5. Browning JD, Horton JD. Molecular mediators of hepatic steatosis and liver injury. J Clin Invest. 2004; 114:147–152. [PubMed: 15254578]
6. Kleiner DE, Brunt EM, Van Natta M, Behling C, Contos MJ, Cummings OW, Ferrell LD, et al. Design and validation of a histological scoring system for nonalcoholic fatty liver disease. Hepatology. 2005; 41:1313–1321. [PubMed: 15915461]
7. Frezza C, Cipolat S, Scorrano L. Organelle isolation: functional mitochondria from mouse liver, muscle and cultured fibroblasts. Nat Protoc. 2007; 2:287–295. [PubMed: 17406588]
8. Hodge AM, English DR, O'Dea K, Sinclair AJ, Makrides M, Gibson RA, Giles GG. Plasma phospholipid and dietary fatty acids as predictors of type 2 diabetes: interpreting the role of linoleic acid. Am J Clin Nutr. 2007; 86:189–197. [PubMed: 17616780]
9. Beysen C, Murphy EJ, Nagaraja H, Decaris M, Riiff T, Fong A, Hellerstein MK, et al. A pilot study of the effects of pioglitazone and rosiglitazone on de novo lipogenesis in type 2 diabetes. J Lipid Res. 2008; 49:2657–2663. [PubMed: 18641372]
10. Argo CK, Northup PG, Al-Osaimi AM, Caldwell SH. Systematic review of risk factors for fibrosis progression in non-alcoholic steatohepatitis. J Hepatol. 2009; 51:371–379. [PubMed: 19501928]
11. Braeuning A, Ittrich C, Kohle C, Hailfinger S, Bonin M, Buchmann A, Schwarz M. Differential gene expression in periportal and perivenous mouse hepatocytes. Febs J. 2006; 273:5051–5061. [PubMed: 17054714]
12. Ratziu V, Giral P, Jacqueminet S, Charlotte F, Hartemann-Heurtier A, Serfaty L, Podevin P, et al. Rosiglitazone for nonalcoholic steatohepatitis: one-year results of the randomized placebo-controlled Fatty Liver Improvement with Rosiglitazone Therapy (FLIRT) Trial. Gastroenterology. 2008; 135:100–110. [PubMed: 18503774]
13. Rinella ME, Elias MS, Smolak RR, Fu T, Borensztajn J, Green RM. Mechanisms of hepatic steatosis in mice fed a lipogenic methionine choline-deficient diet. J Lipid Res. 2008; 49:1068–1076. [PubMed: 18227531]
14. Rinella ME, Green RM. The methionine-choline deficient dietary model of steatohepatitis does not exhibit insulin resistance. J Hepatol. 2004; 40:47–51. [PubMed: 14672613]

15. Ikejima K, Okumura K, Lang T, Honda H, Abe W, Yamashina S, Enomoto N, et al. The role of leptin in progression of non-alcoholic fatty liver disease. Hepatol Res. 2005; 33:151–154. [PubMed: 16198623]

16. Adibi P, Sadeghi M, Mahsa M, Rozati G, Mohseni M. Prediction of coronary atherosclerotic disease with liver transaminase level. Liver Int. 2007; 27:895–900. [PubMed: 17696927]

17. Hanley AJ, Williams K, Festa A, Wagenknecht LE, D'Agostino RB Jr, Kempf J, Zinman B, et al. Elevations in markers of liver injury and risk of type 2 diabetes: the insulin resistance atherosclerosis study. Diabetes. 2004; 53:2623–2632. [PubMed: 15448093]

18. Debois D, Bralet MP, Le Naour F, Brunelle A, Laprevote O. In situ lipidomic analysis of nonalcoholic fatty liver by cluster TOF-SIMS imaging. Anal Chem. 2009; 81:2823–2831. [PubMed: 19296690]

19. Puri P, Baillie RA, Wiest MM, Mirshahi F, Choudhury J, Cheung O, Sargeant C, et al. A lipidomic analysis of nonalcoholic fatty liver disease. Hepatology. 2007; 46:1081–1090. [PubMed: 17654743]

20. Yoshimatsu M, Terasaki Y, Sakashita N, Kiyota E, Sato H, van der Laan LJ, Takeya M. Induction of macrophage scavenger receptor MARCO in nonalcoholic steatohepatitis indicates possible involvement of endotoxin in its pathogenic process. Int J Exp Pathol. 2004; 85:335–343. [PubMed: 15566430]

21. Yamaguchi K, Yang L, McCall S, Huang J, Yu XX, Pandey SK, Bhanot S, et al. Inhibiting triglyceride synthesis improves hepatic steatosis but exacerbates liver damage and fibrosis in obese mice with nonalcoholic steatohepatitis. Hepatology. 2007; 45:1366–1374. [PubMed: 17476695]

22. Bieghs V, Wouters K, van Gorp PJ, Gijbels MJ, de Winther MP, Binder CJ, Lutjohann D, et al. Role of scavenger receptor A and CD36 in diet-induced nonalcoholic steatohepatitis in hyperlipidemic mice. Gastroenterology. 138:2477–2486. e2471–e2473. 2486. [PubMed: 20206177]

23. Angulo P, Keach JC, Batts KP, Lindor KD. Independent predictors of liver fibrosis in patients with nonalcoholic steatohepatitis. Hepatology. 1999; 30:1356–1362. [PubMed: 10573511]

24. Miyaaki H, Ichikawa T, Nakao K, Yatsuhashi H, Furukawa R, Ohba K, Omagari K, et al. Clinicopathological study of nonalcoholic fatty liver disease in Japan: the risk factors for fibrosis. Liver Int. 2008; 28:519–524. [PubMed: 17976158]

25. Balaban RS, Nemoto S, Finkel T. Mitochondria, oxidants, and aging. Cell. 2005; 120:483–495. [PubMed: 15734681]

26. Chowdhry S, Nazmy MH, Meakin PJ, Dinkova-Kostova AT, Walsh SV, Tsujita T, Dillon JF, et al. Loss of Nrf2 markedly exacerbates nonalcoholic steatohepatitis. Free Radic Biol Med. 2010; 48:357–371. [PubMed: 19914374]

27. Sugimoto H, Okada K, Shoda J, Warabi E, Ishige K, Ueda T, Taguchi K, et al. Deletion of nuclear factor-E2-related factor-2 leads to rapid onset and progression of nutritional steatohepatitis in mice. Am J Physiol Gastrointest Liver Physiol. 2010; 298:G283–G294. [PubMed: 19926817]

28. Tanaka Y, Aleksunes LM, Yeager RL, Gyamfi MA, Esterly N, Guo GL, Klaassen CD. NF-E2-related factor 2 inhibits lipid accumulation and oxidative stress in mice fed a high-fat diet. J Pharmacol Exp Ther. 2008; 325:655–664. [PubMed: 18281592]

29. Ratziu V, Charlotte F, Bernhardt C, Giral P, Halbron M, Lenaour G, Hartmann-Heurtier A, et al. Long-term efficacy of rosiglitazone in nonalcoholic steatohepatitis: Results of the fatty liver improvement by rosiglitazone therapy (FLIRT 2) extension trial. Hepatology. 2009; 51:445–453. [PubMed: 19877169]

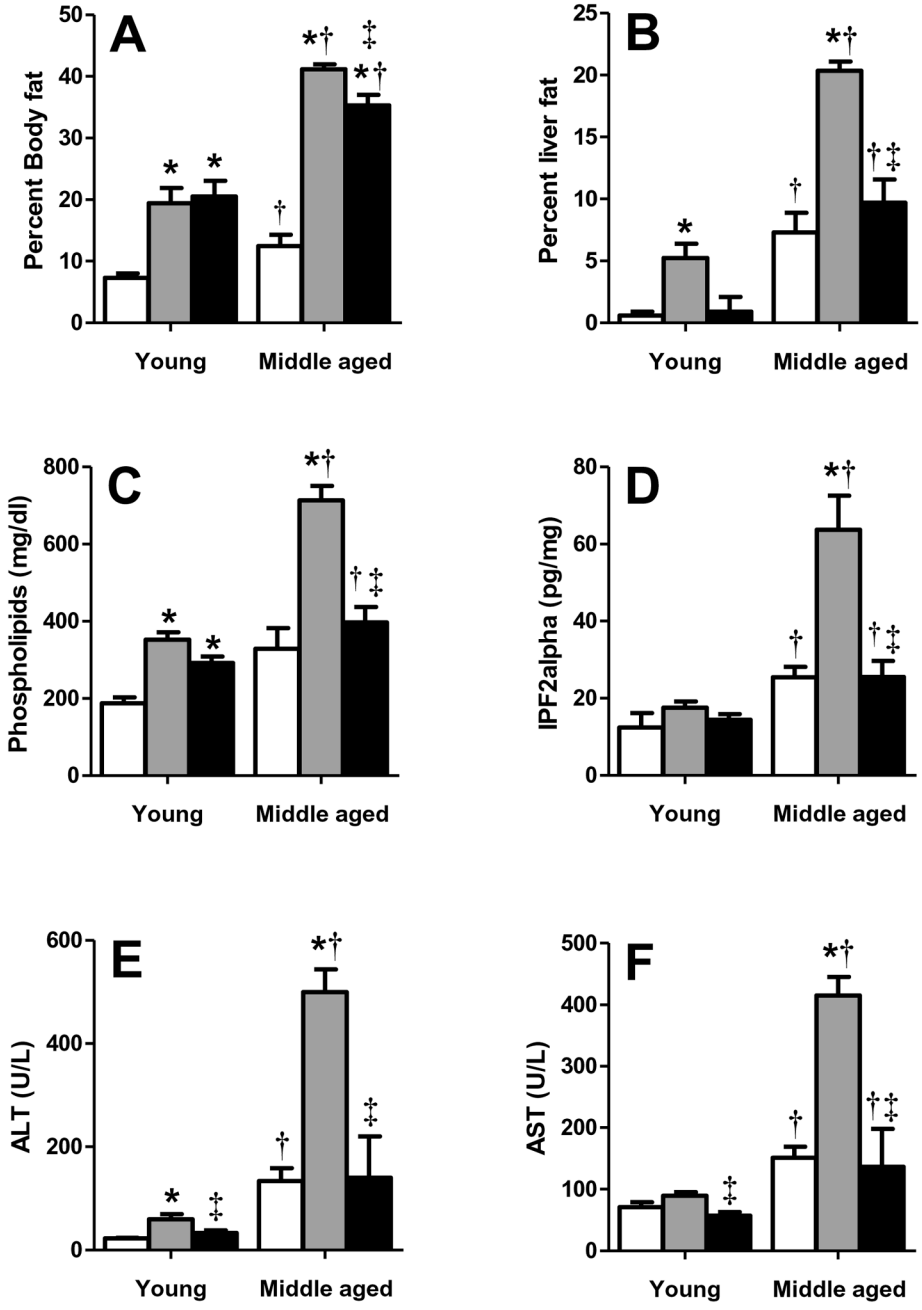

Figure 1. MS mice have aggravated liver fat, oxidative stress and injury

Young and middle-aged *LDLR*$^{-/-}$ mice fed chow (white), HFD (grey), or HFD+RSG (black bars) for 12 weeks were analyzed to determine percent (A) body and (B) liver fat and plasma (C) phospholipids, and (D) F2α isoprostane, (E) ALT and (F) AST levels. (Mean ±SE; N=4–10/group; *P<0.05 vs. age-matched chow; †P<0.05 vs. matching diet; and ‡P<0.05 vs. age-matched HFD by Student's t-test).

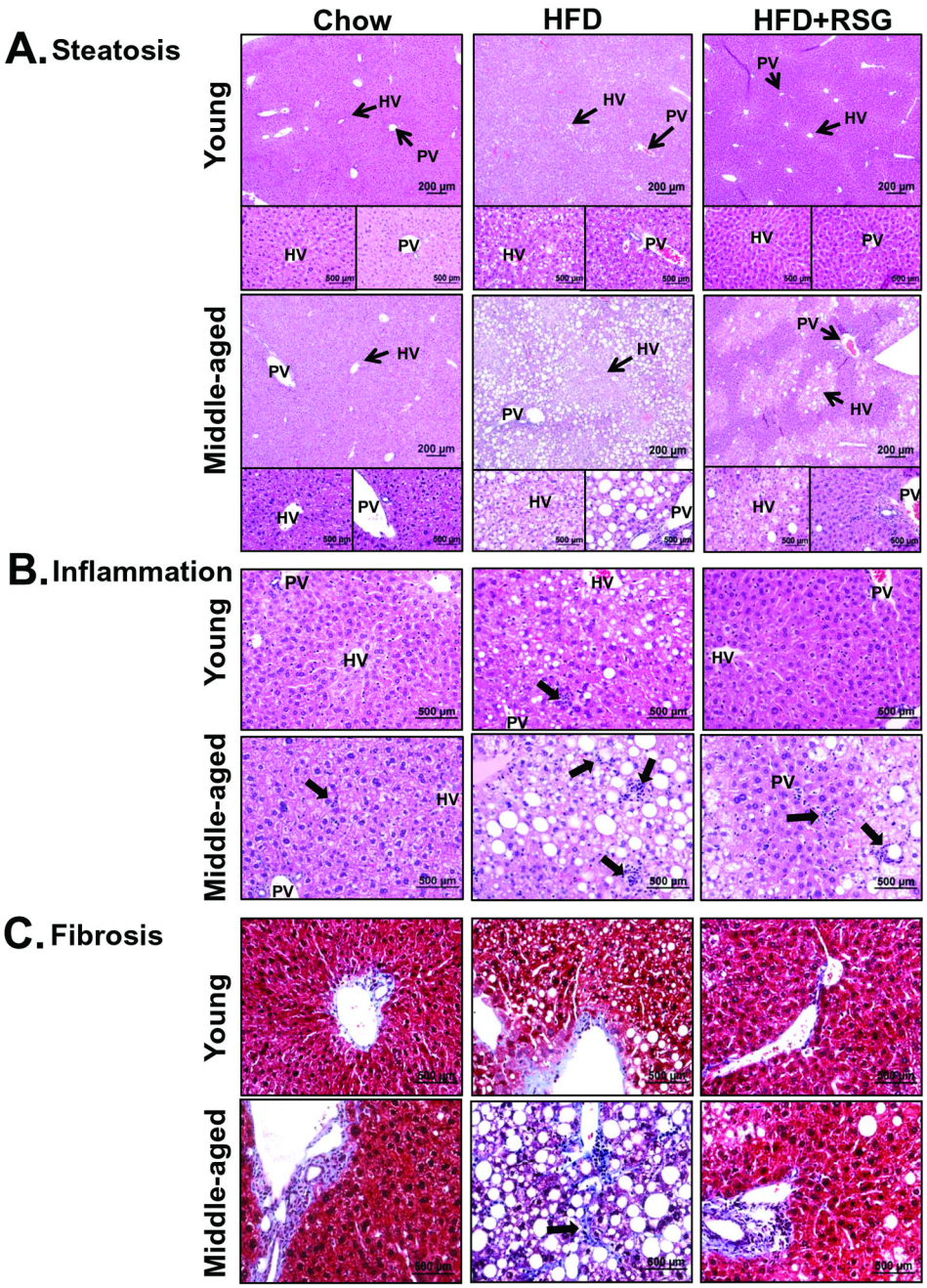

Figure 2. MS mice develop histological features of NASH

LDLR$^{-/-}$ mouse liver sections were analyzed for age- and diet-associated effects on (A) liver steatosis, (B) inflammation by contrast staining with Haematoxylin and Eosin, while effects on (C) fibrosis were analyzed using Masson's trichrome to detect collagen (blue color). Insets show magnified images. Arrows indicate (A) hepatic (HV) and portal veins (PV), (B) inflammatory foci, or (C) sinusoidal fibrosis.

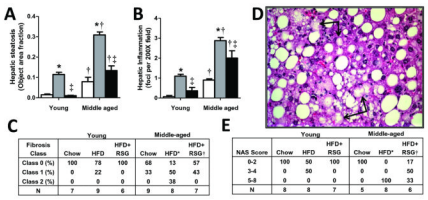

Figure 3. RSG decreases NASH

LDLR$^{-/-}$ mouse liver sections were analyzed for (A) steatosis area, (B) inflammatory foci and (C) fibrosis area, which was classified as class 0 (none), 1 (periportal OR sinusoidal), 2 (periportal AND sinusoidal) or 3 (bridging fibrosis). (A–B: Mean±SE; N=6–9/group. *P<0.05 vs. age-matched chow; †P<0.05 vs. matching diet; and ‡P<0.05 vs. age-matched HFD by Student's t-test). (D) MS mice developed ballooning degeneration. (E) NAS summary scores. (C, E: *P<0.05 vs. HFD-fed mice, †P<0.05 vs. HFD+RSG-fed mice by Chi-square for trend).

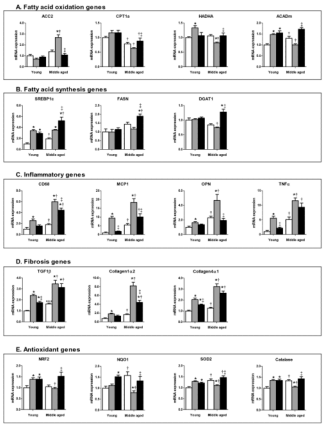

Figure 4. Gene expression changes in livers of MS mice

Liver GAPDH-normalized (A) *ACC2*, *CPT1A*, *HADHA*, *ACADm*, (B) *SREBP1c*, *FASN*, *DGAT1*, (C) *CD68*, *MCP1*, *OPN*, *TNFα*, (D) *TGF1β*, *Collagen1α2*, *Collagen4α1*, (E) *NRF2*, *NQO1*, *SOD2*, Catalase mRNA expression for chow-fed (white), HFD-fed (grey) and HFD +RSG-treated (black) young and middle-aged *LDLR*$^{-/-}$ mice. (Means±SE; N=4–9/group. *P<0.05 vs. age-matched chow; †P<0.05 vs. matching diet; and ‡P<0.05 vs. age-matched HFD by Student's t-test).

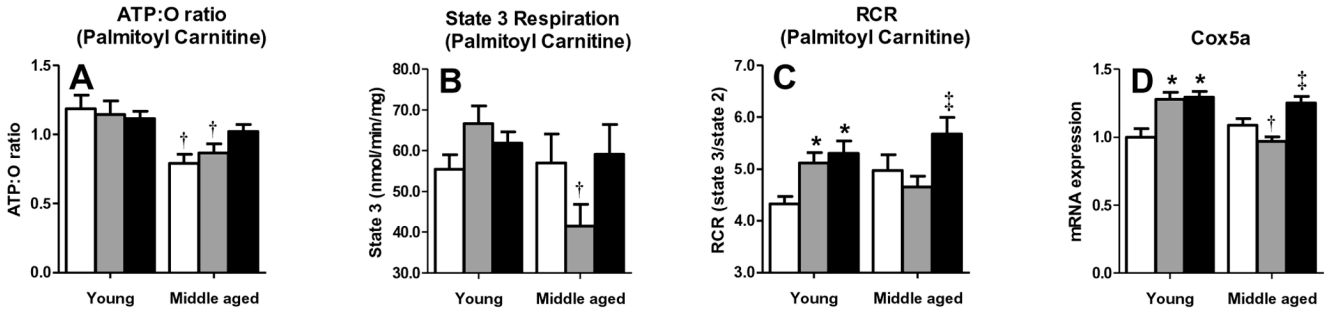

Figure 5. Rosiglitazone improves liver mitochondrial function in MS mice

Liver mitochondria responses to ADP and palmitoyl carnitine are shown. ATP:O ratios were calculated from the change in O_2 concentrations during state 3 (150 μM ADP). (A) ATP:O ratio, (B) state 3 respiration, (C) RCR (state 3/state 2) for mitochondria isolated from chow-fed (white), HFD-fed (grey) and HFD+RSG-treated (black) young and middle-aged *LDLR*$^{-/-}$ mice. (D) Liver Expression of mitochondrial gene *Cox5a*. (Means±SE; N=5–7/group. *P<0.05 vs. age-matched chow; †P<0.05 vs. matching diet; and ‡P<0.05 vs. age-matched HFD by Student's t-test).

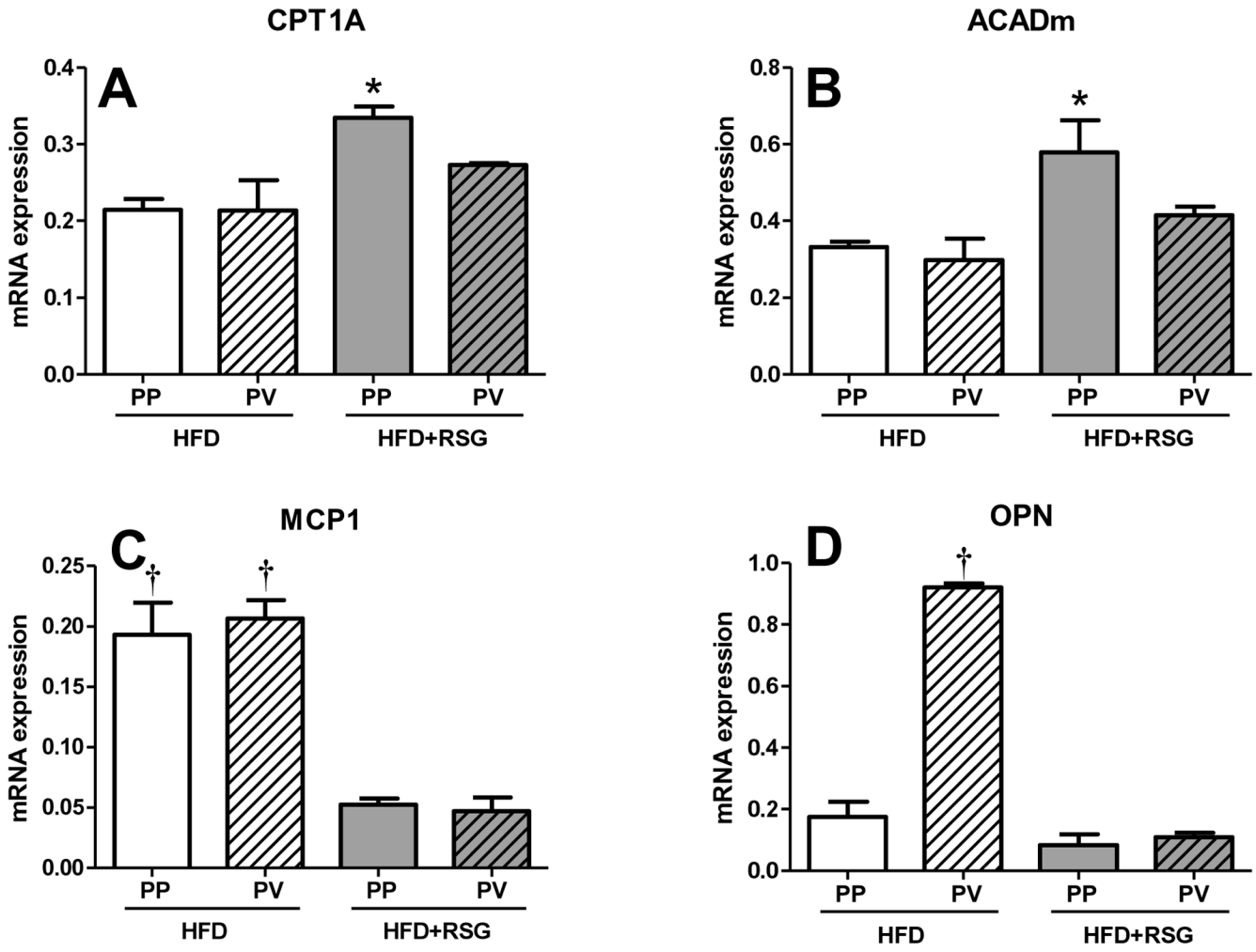

Figure 6. RSG has differential effects on periportal and perivenous regions of the liver

RT-PCR analysis of laser capture microdissection samples of periportal and perivenous regions of the liver parenchyma for β-oxidation-related (A) *CPT1A*, (B) *ACADm* and proinflammatory (C) *MCP1* and (D) *OPN* gene expression. In HFD-fed mice, periportal regions (PP, defined as the region surrounding the portal vein) were predominantly macrosteatotic and perivenous regions (PV, defined as the area around the hepatic vein) were primarily microsteatotic. (Means±SE; N=3/group. *P<0.05 vs. all other groups; †P<0.01 vs. matching HFD+RSG samples by Student's t-test).

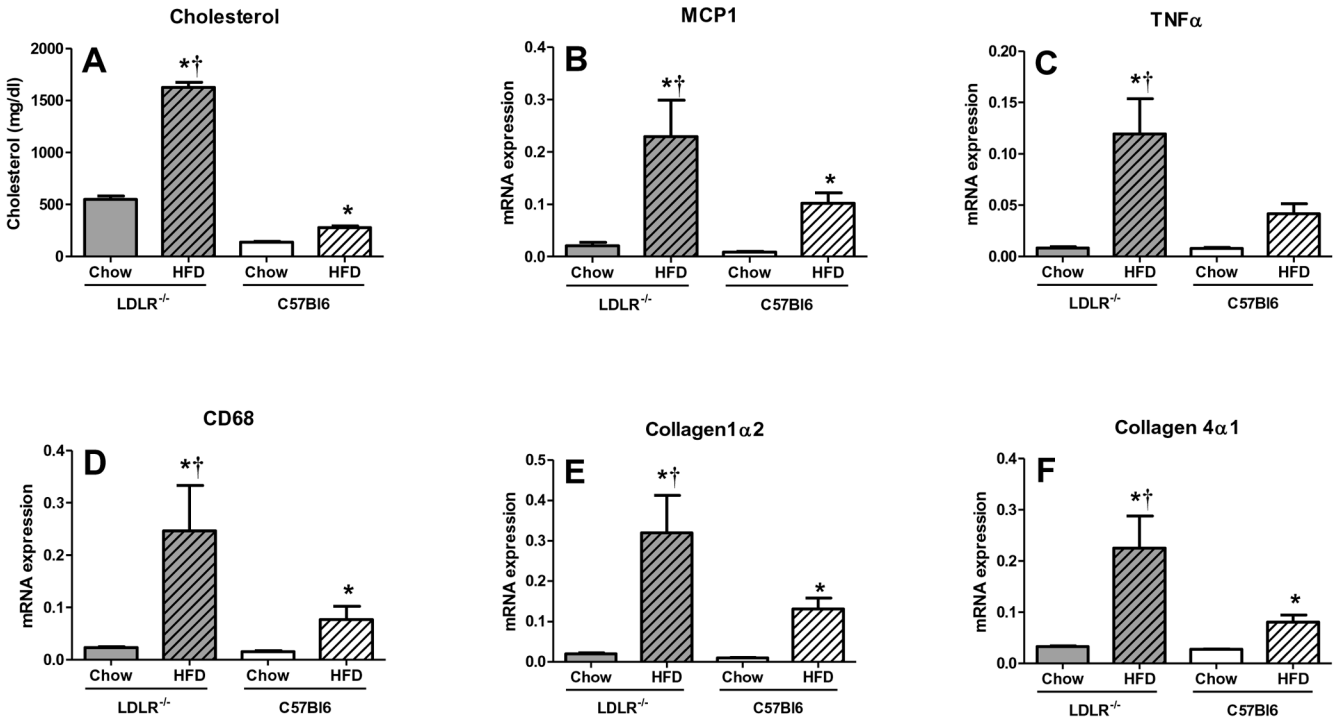

Figure 7. *LDLR*$^{-/-}$ mice have more liver inflammation than age-matched C57BL6 mice fed HFD

Middle-aged C57BL/6 and *LDLR*$^{-/-}$ mice were fed chow or HFD for 3 months (A) Plasma cholesterol levels and liver inflammatory (B) *MCP1*, (C) *TNFα*, (D) *CD68* and fibrotic (E) *Collagen 1α2* and (F) *Collagen 4α1* gene expression was greater in HFD-fed *LDLR*$^{-/-}$ vs. age-matched C57BL6 mice. (Means±SE; N=8–10/group. *P<0.05 vs. genotype-matched chow; †P<0.05 vs. all other groups by Student's t-test).